

# Measurement of monoterpenes and related compounds by proton transfer reaction-mass spectrometry (PTR-MS)

A. Tani<sup>a,b</sup>, S. Hayward<sup>a</sup>, C.N. Hewitt<sup>a,\*</sup>

<sup>a</sup> Department of Environmental Science, Institute of Environmental and Natural Sciences,  
Lancaster University, Lancaster LA1 4YQ, UK

<sup>b</sup> School of High-Technology for Human Welfare, Tokai University, 317 Numazu, Shizuoka 410-0395, Japan

Received 1 February 2002; accepted 10 June 2002

In memoriam Werner Lindinger.

## Abstract

The reactions of monoterpenes and related C<sub>10</sub> compounds with H<sub>3</sub>O<sup>+</sup> in a proton transfer reaction-mass spectrometer (PTR-MS) were studied, with a view to better understanding the signal produced by this instrument when detecting these compounds. The monoterpenes α- and β-pinene, 3-carene and limonene produced fragment ions of masses 67, 81 and 95 as well as a protonated molecular ion of mass 137, while *p*-cymene (C<sub>10</sub>H<sub>14</sub>) produced ions of masses 41, 91, 93 and 119 in addition to mass 135. The fragmentation patterns were observed to vary as *E/N* was varied. Camphor (C<sub>10</sub>H<sub>16</sub>O) did not fragment within the *E/N* range 80–120 Td. The proton transfer reaction rate coefficients for these monoterpene species with H<sub>3</sub>O<sup>+</sup> were found to be  $2.2 \times 10^{-9}$  to  $2.5 \times 10^{-9}$  cm<sup>3</sup> s<sup>-1</sup>. For camphor the rate coefficient was  $4.4 \times 10^{-9}$  cm<sup>3</sup> s<sup>-1</sup>. Water vapour pressure in the inlet air affected the fragmentation pattern for *p*-cymene, limonene and 3-carene. The uncertainties associated with the PTR-MS measurement of these compounds are discussed. (Int J Mass Spectrom 223–224 (2003) 561–578) © 2002 Elsevier Science B.V. All rights reserved.

**Keywords:** Monoterpenes; GC-FID; Proton transfer reaction-mass spectrometry, PTR-MS

## 1. Introduction

Many compounds in the monoterpene family (C<sub>10</sub>H<sub>16</sub>) are produced by tree species and emitted into the atmosphere as a result of their volatilities. They represent a significant fraction of the total volatile organic compound (VOC) flux from the biosphere to the atmosphere. Their mechanisms of formation and rates of emission, plus their roles in atmospheric chemistry, are reviewed extensively by

Fall [1] and Fehsenfeld et al. [2], respectively, and elsewhere.

Measurement of the atmospheric concentrations and biogenic emission rates of the monoterpenes and related VOCs are necessary if their roles in plant biochemistry, plant physiology and atmospheric chemistry are to be understood and quantified. However, the low concentrations and emission rates of these compounds renders their analysis difficult, relying until recently on their preconcentration with subsequent off-line analysis by gas chromatography with, typically, flame ionisation or mass spectrometric detection.

\* Corresponding author. E-mail: n.hewitt@lancaster.ac.uk

Recently, proton transfer reaction-mass spectrometry (PTR-MS), using protonated water ( $\text{H}_3\text{O}^+$ ) as the primary ionising reactant, has been developed, allowing the on-line monitoring of VOCs, including the monoterpenes and related compounds [3]. Other applications have included monitoring changes in the composition of human breath [4] and in urban [5] and rural [6] air.

The transfer of protons from  $\text{H}_3\text{O}^+$  to neutral entities can be regarded as a 'soft' ionisation and, under 'normal' PTR-MS operating conditions (detailed below), many VOCs are detected as their molecular mass plus one. However, some compounds, including the monoterpenes, are observed to undergo some degree of fragmentation within the instrument. Holzinger et al. [7] reported that the monoterpenes undergo some fragmentation, yielding product ions of mass 137 (33%) and 81 (67%) at drift tube conditions of 130 Td (Td = Townsend;  $1 \text{ Td} = 10^{-17} \text{ V cm}^2 \text{ mol}^{-1}$ ). The Townsend is a measure of  $E/N$  (where  $E$  is the electric field strength and  $N$  the buffer gas number density) within the drift tube, and this fragmentation is dependent on the  $E/N$  value and the mean relative centre-of-mass kinetic energy ( $\text{KE}_{\text{ion}}$ ). The fragment pattern may vary between individual monoterpene species because their physico-chemical properties, such as proton affinity, are different. Since PTR-MS measures the total concentration of all monoterpenes (it does not allow for preliminary compound separation as in GC-FID, for example), it may be helpful to determine the representative fragment pattern of typical monoterpene mixtures observed in plant emissions, as well as individual monoterpene fragment patterns, as a function of  $E/N$ .

A potential source of inaccuracy during PTR-MS measurement of the monoterpenes is uncertainty in the values used for the proton transfer reaction rate coefficients of individual species with the  $\text{H}_3\text{O}^+$  ions. These can be estimated using the parameterised trajectory formulation developed by Su and Chesnavich [8] if the dipole moment and polarisability of the compound of interest are known. There is, however, only limited information available regarding these properties for the monoterpenes [9]. As a result, a nominal value

of  $2.0 \times 10^{-9} \text{ cm}^3 \text{ s}^{-1}$  has previously been adopted for the PTR-MS quantification of monoterpenes (Ionicon, personal communication). Since individual monoterpenes may have different rate coefficients, owing to their different physico-chemical properties, it is highly desirable to determine the rate coefficients for individual monoterpene species to allow correct quantification of measured concentrations.

In this paper, we use PTR-MS to investigate the fragmentation patterns of four compounds in the monoterpene family ( $\alpha$ - and  $\beta$ -pinene, 3-carene and limonene ( $\text{C}_{10}\text{H}_{16}$ )), plus two compounds related to the monoterpenes ( $p$ -cymene ( $\text{C}_{10}\text{H}_{14}$ ) and the oxygenate camphor ( $\text{C}_{10}\text{H}_{16}\text{O}$ )), and show how the fragmentation pattern of each individual compound is affected by  $E/N$  in the drift tube. We have chosen these compounds because they are known to be important in the spectrum of VOCs produced by trees [1]. Using a relative rate coefficient determination method with simultaneous GC-FID quantification of gaseous standards at varying concentrations, we obtain proton transfer reaction rate coefficients for the six compounds with  $\text{H}_3\text{O}^+$  ions. We also show how the fragment constituents are affected by water vapour pressure in the sample air introduced into the PTR-MS. This reveals a need for a humidity correction for  $p$ -cymene measurement. Using these reaction data, we determine the concentrations of monoterpenes in a glass vessel in which damaged branches of Sitka spruce are incubated, to determine how a detailed knowledge of VOC behaviour in the PTR-MS can aid signal deconvolution and compound quantification. Finally we discuss the uncertainties associated with PTR-MS measurements, by comparing them with concentrations simultaneously obtained by GC-FID.

## 2. Experimental methods

### 2.1. PTR-MS instrumentation

The PTR-MS (Ionicon GmbH, Innsbruck) has been described in detail elsewhere [3,4]; therefore only the points relevant to this paper are given here. The

PTR-MS consists of three parts: an ion source, a drift tube (reaction chamber) and an ion separation/detection system.  $\text{H}_3\text{O}^+$  ions formed in the hollow cathode ion source react with neutrals (R) in the drift tube, undergoing proton transfer reactions. The resultant product ions ( $\text{RH}^+$ ) are separated by a quadrupole mass spectrometer (Balzers QMG421) and detected as ion counts per second (cps) by a secondary electron multiplier (Balzers QC422). The signals are corrected for instrumental transmission coefficients.

$\text{H}_3\text{O}^+$  ions may also become hydrated to produce  $\text{H}_3\text{O}^+\text{H}_2\text{O}$  cluster ions, although under the ‘normal’ operating conditions described herein (relative humidity of 20–30%, an ambient temperature of  $21 \pm 1^\circ\text{C}$ , and a drift tube  $E/N$  of 120 Td), the ratio of the densities of  $\text{H}_3\text{O}^+\text{H}_2\text{O}$  to  $\text{H}_3\text{O}^+$  in the drift tube is usually less than 3%. The  $E/N$  range between 120 and 140 Td has been regarded as a compromise between minimising water cluster ion formation, which could obscure the mass spectra, and suppression of product ion fragmentation which would complicate the identification of the target analytes [3]. Since the density of  $\text{H}_3\text{O}^+$  ions,  $[\text{H}_3\text{O}^+]$ , is high in the drift tube, and only a small fraction of the  $\text{H}_3\text{O}^+$  ions reacts with the neutrals,  $[\text{H}_3\text{O}^+]$  remains constant and pseudo-first order reaction kinetics are maintained. Under these conditions, the density of product ions  $[\text{RH}^+]$  is given by:

$$[\text{RH}^+] \approx [\text{H}_3\text{O}^+][\text{R}]kt \quad (1)$$

where  $[\text{H}_3\text{O}^+]$  is the density of  $\text{H}_3\text{O}^+$ ,  $[\text{R}]$  the molecular ion density of trace component R,  $k$  the reaction

rate coefficient for the proton transfer reaction between R and  $\text{H}_3\text{O}^+$  and  $t$  the time taken for  $\text{H}_3\text{O}^+$  ions to traverse the drift tube. The  $k$  values are available for a number of compounds [10], typically in the range  $1.5 \times 10^{-9}$  to  $4.0 \times 10^{-9} \text{ cm}^3 \text{ s}^{-1}$ , but there is no information available for the monoterpenes. The Langevin rate coefficient  $k_L$  and ion capture rate coefficient  $k_c$ , which are calculated from estimated or measured polarisability and dipole moment [8], can provide estimates ( $\pm 30\%$ ) of reaction rate coefficients for such proton transfer processes. However, there is no information available for the monoterpene family, except for  $\alpha$ -pinene, limonene and camphor [9]. A selection of  $k_c$  and  $k_L$  values for these compounds is presented in Table 1 (columns 7 and 8) and ranges from  $2.4 \times 10^{-9}$  to  $4.4 \times 10^{-9} \text{ cm}^3 \text{ s}^{-1}$ .

## 2.2. Standard preparation by diffusion system

In order to identify individual monoterpene fragment patterns, to investigate the effects of collisional energy on these fragmentation patterns, and to determine the rate coefficients experimentally, a diffusion system was constructed. A range of nominal gaseous concentrations can be produced with this system (Fig. 1). Two air streams, dried by  $\text{CaSO}_4$  and purified by charcoal filtration, were regulated by mass flow controllers ( $0.5\text{--}5 \text{ L min}^{-1}$ , MKS Instruments, USA). One of the air streams passed through a temperature controlled ( $5\text{--}85^\circ\text{C}$ , with an accuracy of  $\pm 0.1^\circ\text{C}$ ) monoterpene diffusion system, whilst the other acted

Table 1  
Proton transfer reaction rate coefficients,  $k$ , obtained from the relative determination method using toluene

Molecule	$m$ (u)	$\alpha$ ( $10^{-24} \text{ cm}^3$ )	$\mu$ (D)	$k$ ( $10^{-9} \text{ cm}^3 \text{ s}^{-1}$ )	$k_L$ ( $10^{-9} \text{ cm}^3 \text{ s}^{-1}$ )	$k_c$ ( $10^{-9} \text{ cm}^3 \text{ s}^{-1}$ )
$\alpha$ -Pinene ( $\text{C}_{10}\text{H}_{16}$ )	136	$17 \pm 1$	0.6	2.2	2.36	2.54
$\beta$ -Pinene ( $\text{C}_{10}\text{H}_{16}$ )	136	$17 \pm 1$	–	2.3	2.36	–
Limonene ( $\text{C}_{10}\text{H}_{16}$ )	136	$17 \pm 1$	1.57	2.3	2.36	3.06
3-Carene ( $\text{C}_{10}\text{H}_{16}$ )	136	$17 \pm 1$	–	2.2	2.36	–
<i>p</i> -Cymene ( $\text{C}_{10}\text{H}_{14}$ )	134	$17 \pm 1$	0	2.5	2.37	2.37
Camphor ( $\text{C}_{10}\text{H}_{16}\text{O}$ )	152	$18 \pm 1$	3.1	4.4	2.42	4.43
Toluene ( $\text{C}_7\text{H}_8$ )	92	12.3	0	2.2	2.07	2.17

$k_L$  and  $k_c$  are the Langevin ion capture rate coefficient and the collisional rate coefficient calculated from the molecular mass,  $m$ , polarisability,  $\alpha$ , and dipole moment,  $\mu$ , using the parameterised trajectory formulation of Su and Chesnavich [8]. The values of  $\alpha$  and  $\mu$  shown in regular type are the known values obtained from [9]. The values shown in italic type are estimated from the known values for similar molecules.

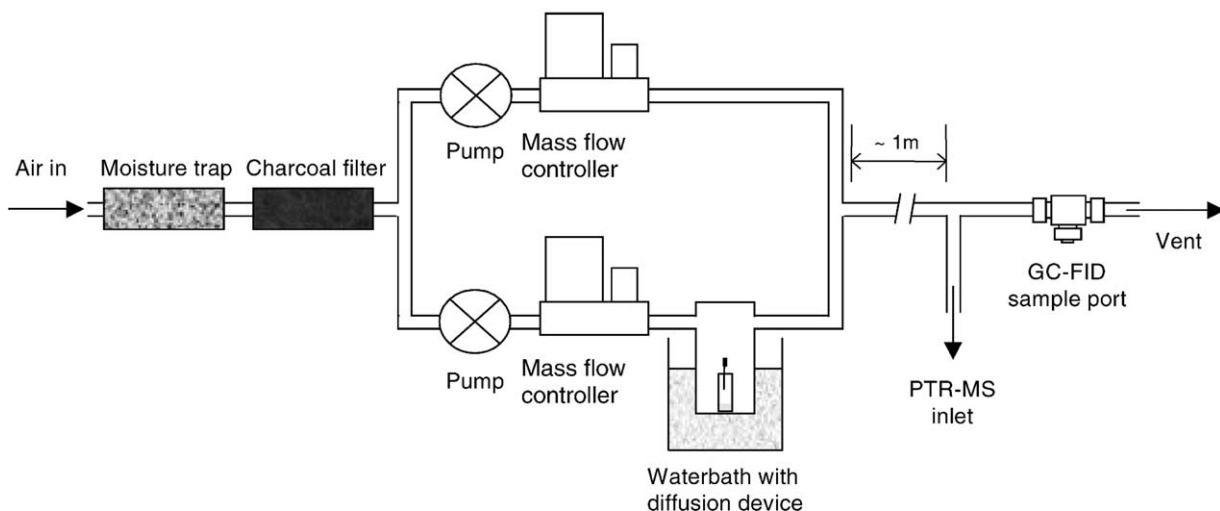


Fig. 1. Schematic diagram of the diffusion system used to generate monoterpene atmospheres of variable concentration.

as a bypass. The diffusion system consisted of a glass chamber ( $\sim 100$  mL) housing a sealed vial (1.5 mL) containing 10–20  $\mu\text{L}$  of a pure monoterpene standard. The septum of the vial was pierced by a syringe, enabling monoterpene vapour to diffuse out at a constant nominal rate into the air stream. The resultant air stream was subsequently combined with the bypass air stream, mixed over a length of  $\sim 1$  m and sampled by PTR-MS, and/or onto solid adsorbent sample tubes for GC-FID analysis. Monoterpene concentrations in the ppbv–ppmv ( $10^{-9}$ – $10^{-6}$  volume mixing ratio) range were achieved by manipulation of the two air flow rates and the water bath temperature.

Monoterpene standards of high purity were obtained commercially.  $\alpha$ -Pinene,  $\beta$ -pinene and camphor (Aldrich, UK) were 98, 99, and 96% pure respectively. Limonene, 3-carene and *p*-cymene (Fluka, UK) were 99, 99 and 95% pure respectively. The impurities of the pure standards are of particular concern since they can interfere with identification of the true fragmentation patterns of individual compounds. If the volatilities of the impurities are greater than that of the standard itself, their abundances will be exaggerated in the vapour phase (when compared with the liquid phase) and resultant mass spectrum, giving an

incorrect fragmentation pattern. To overcome these problems, steps were taken to discriminate between the contribution of each standard and its impurities to the mass spectrum. These are detailed below.

### 2.3. PTR-MS operation

Sample air containing variable amounts of monoterpenes was introduced to the PTR-MS drift tube via a  $\sim 1$  m length of 1/8 in. o.d. PFA tubing at a flow rate of 7–11.8  $\text{mL min}^{-1}$ . To assess fragmentation patterns, the  $E/N$  of the drift tube was increased to 170 Td and decreased to 80 Td from the normal value of 120 Td by altering the drift tube voltage and pressure, respectively. The mean relative centre-of-mass kinetic energies,  $KE_{\text{ion}}$ , calculated from ion mobility data [11] were found to be 0.09, 0.22 and 0.45 eV for  $E/N$  values of 80, 120 and 170 Td, respectively.

Water vapour pressure was found to be linearly correlated with the signal of mass 37 ( $\text{H}_3\text{O}^+\text{H}_2\text{O}$ ) at an  $E/N$  of 120 Td and with the signal of mass 55 ( $\text{H}_3\text{O}^+(\text{H}_2\text{O})_2$ ) at an  $E/N$  of 80 Td. These masses were therefore monitored continuously. Even at zero relative humidity in the inlet air, a small amount of water exists in the drift tube, from the ion source [5].

By extrapolating the linear relationships to the points where the  $\text{H}_3\text{O}^+\text{H}_2\text{O}$  signal was zero, the water vapour density entering from the ion source was calculated to be equivalent to 20% relative humidity when the sample air temperature was 21 °C.

#### 2.4. Gas sampling and GC analysis

Air samples were periodically collected on dual bed stainless steel sample tubes (Perkin-Elmer) containing Tenax-TA (200 mg) and Carbotrap (100 mg). Sample tubes were pre-conditioned at 280 °C for 30 min in a stream of purified helium at 50 mL min<sup>-1</sup> and were sealed and stored at 4 °C until sampling. Samples were collected at a flow rate of 200 mL min<sup>-1</sup> via a length of 1/4 in. o.d. PFA tubing. Sample duration was dependent on the vapour concentration, e.g., 2 min for 100 ppbv and 60 min for 5 ppbv, to ensure the amount adsorbed remained within the range of standards. Calibration standards were prepared by diluting pure compounds in methanol and injecting aliquots onto preconditioned sample tubes in a stream of purified helium.

Impurities in the standard vapours and solutions, and natural VOC emissions from a plant, were identified by GC-MS (Hewlett-Packard 5890 GC-5870 MS) and quantified by GC-FID (Perkin-Elmer Autosystem). In both systems, samples underwent two stage thermal desorption (Perkin-Elmer ATD 400) and compound separation was achieved using an Ultra-2 capillary column (Hewlett-Packard). GC analytical procedures and parameters are described in detail elsewhere [12]. The detection limit ( $S/N = 3$ ) of the GC-FID system was 0.03–0.04 pmol on column.

#### 2.5. Identification of ions derived from standards and impurities

A monoterpene concentration in the gas phase of 100–300 ppbv was produced and the PTR-MS operated in the scan mode to select all ions produced in the mass range 21–200 (including ions derived from any impurities present). The ions present for which the signal exceeded 0.1% of the signal of the dominant

ion were selected, and in the subsequent experiments the PTR-MS was tuned to detect them only.

The ions in the PTR-MS spectrum of each monoterpene originating from impurities in the standards were identified using three complementary methods: GC-MS/FID analysis of diluted standard vapours and solutions, correlation analysis between individual ions measured by PTR-MS, at various concentrations of standard vapours (obtained by varying the water bath temperature), and PTR-MS measurements at increased and decreased  $E/N$  values in the drift tube (i.e., varying compound fragmentation).

#### 2.6. Determination of reaction rate coefficient

The reaction rate coefficients of individual monoterpenes with  $\text{H}_3\text{O}^+$  ions at normal PTR-MS operating conditions were determined from Eq. (1). The concentration of the neutral  $[R]$  was simultaneously measured by GC-FID. To determine the reaction time  $t$  and evaluate the overall accuracy of the measurement system, the concentration of toluene in a test atmosphere was determined by PTR-MS and GC-FID simultaneously. Toluene was used as its rate coefficient with  $\text{H}_3\text{O}^+$  is known ( $2.2 \times 10^{-9} \text{ cm}^3 \text{ s}^{-1}$ ) and the measurement of toluene by PTR-MS has been well characterised and documented (e.g. [5]).

To measure the concentrations of the monoterpene family with GC-FID and to calculate the proton transfer reaction rate coefficient, we collected 7–12 samples at different vapour concentrations (5–500 ppbv). As a result of their ‘sticky’ nature, vapours were not sampled unless their signal measured by PTR-MS reached a steady state following a change in water bath temperature and/or flow rates of the diffusion system.

#### 2.7. Water vapour control experiment

To investigate the effect of water vapour pressure on PTR-MS measurement of the monoterpene family, we varied water vapour pressure in the diluted standard vapours whilst maintaining their concentration at constant levels. A dew point generator (LI-610, LI-COR,

USA) was installed between the charcoal filter and mass flow controller of the diffusion system (Fig. 1), and the water vapour pressure in the air introduced into the diffusion system glass chamber was varied. For this experiment, the pumps and bypass line shown in Fig. 1 were not used. The air flow through the system was maintained by a pump built into the dew point generator, and regulated with the mass flow controller at a flow rate of  $1 \text{ L min}^{-1}$ , before being diverted through the diffusion chamber and introduced to the PTR-MS inlet. Water vapour pressure of the air was varied from 0.7 to 2.5 kPa, which is equivalent to a RH of 28–98%. The compounds in the monoterpene family were monitored by PTR-MS across this humidity range. The  $E/N$  of the drift tube was usually maintained at normal conditions but was occasionally switched to 80 Td.

### 2.8. Plant wounding experiments

To compare the concentrations measured with PTR-MS and GC-FID and to evaluate the feasibility of monoterpene measurement in “real” samples with PTR-MS, we measured natural VOC emissions, using both techniques, from a Sitka spruce (*Picea sitchensis*) specimen following wounding. Sitka spruce is a known monoterpene emitter [12], and wounding enhances the emission rate of VOC compounds and induces the emission of other specific “wound response” compounds [13]. A 5 cm branch was excised from a 130 cm tall seedling, and cut into three pieces prior to the start of measurement. The three pieces were immediately put into a glass vessel (50 mL) which was fitted with inlet and outlet ports. The glass vessel was placed in a water bath, and an air flow was directed through the vessel using the apparatus detailed in Fig. 1. Ions indicative of the monoterpene family, plus those of the hexenal and hexanal families [13], were monitored on-line with PTR-MS over a period of  $\sim 2 \text{ h}$ . Drift tube  $E/N$  was maintained at normal conditions except for two periods (10 min each) when it was temporarily reduced to 80 Td. In addition, air samples were simultaneously collected onto dual bed sample tubes for subsequent GC-FID analysis ( $n = 7$ ).

## 3. Results and discussion

### 3.1. Effect of $E/N$ on fragment pattern using pure monoterpene standards

Several impurities in the standard solutions and their vapours were identified by GC-MS, and were dominated by  $\text{C}_{10}$ -alkylbenzenes and other monoterpene species. The total GC-FID peak area of impurity vapours was less than 5% in all cases except for that of 3-carene, for which impurities, including  $\text{C}_{10}$  alkylbenzenes and  $\alpha$ -phellandrene, totaling 8% were found in the vapour phase.

Varying the water bath temperature was found to be effective in distinguishing between fragment ions derived from standards and those originating from impurities. Since the vapour pressure varies as a function of temperature, and the functions differ among compounds, fragment ions derived from standards should increase proportionally to their protonated molecular ion as temperature is increased. As a result, they are distinguishable from impurities. Using this technique, ions identified as impurities were masses 71, 93, 97, 109 and 119 for monoterpene standards, masses 51 and 99 for *p*-cymene and 57, 59, 81 and 117 for camphor. However, the signal of mass 93 in the  $\alpha$ -pinene and 3-carene measurements was relatively large, i.e., 0.5–1% of that of mass 81 + 137. This raises the possibility that even if a fragment ion of mass 93 does originate from the pure standards, it may be masked by the relatively abundant impurities. However, if this is the case, the abundance of the monoterpene-derived mass 93 must be less than 0.5% of the total signal of ions derived from these monoterpenes. Fig. 2 shows the relationship between the signal of mass 137 and those of major ions observed in the vapour of the 3-carene standard, including some impurities. This illustrates the different volatilities of 3-carene and its impurities, and shows how this method can easily be used to identify impurities in standard compounds.

Decreasing  $E/N$  in the drift tube increased the abundance of protonated molecular ions, both of standard and impurity compounds. Ions of mass 135 derived from  $\text{C}_{10}$  alkylbenzene impurities in the monoterpene



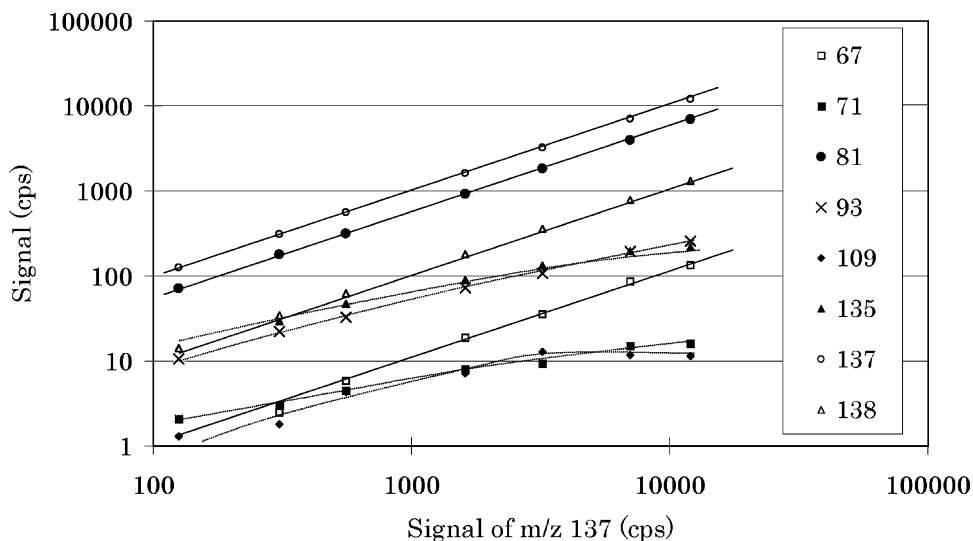


Fig. 2. Relationship between the *signal* of mass 137 (the protonated non-isotopic molecular ion) and the signals of other major ions observed in the vapour phase of a 3-carene standard containing some impurities. Different concentrations in the vapour phase were obtained by varying the water bath temperature (20–70°C). The *signal* of ions derived from 3-carene show constant ratios to the mass 137 *signal* across the entire concentration range (solid lines) whilst those attributable to impurities show some deviations (dashed lines), owing to their differing volatilities. In this figure, only the major ions are shown. Those derived from impurities are masses 69, 71, 93, 109 and 135, whilst those derived from 3-carene are masses 67, 81, 137 and 138.

standards were less than 3% of mass 137 at a drift tube  $E/N$  of 80 Td and easily distinguished. For *p*-cymene (protonated non-isotopic molecular mass 135) and camphor (protonated non-isotopic molecular mass 153), other protonated ions such as monoterpenes (mass 137) were also identified. For limonene, *p*-cymene and camphor,  $E/N$  was increased to 170 Td by decreasing the drift tube pressure. In addition to varying water bath temperature, this is also a useful method of identifying fragment ions derived from the standards, because the enhanced fragmentation at high  $E/N$  facilitates ion identification: if the fractional signal of an ion exceeds the fraction of impurity present in the vapour phase, this indicates that the ion is derived, at least in parts, from monoterpene standard compound. Masses 67 and 95 for limonene and masses 91 and 119 for *p*-cymene showed enhanced signals at high  $E/N$  (170 Td), above the fractional impurity concentration, indicating that these ions were derived from the standard compounds.

Using above techniques, all four monoterpenes investigated with PTR-MS were found to produce frag-

ment ions of masses 67, 81 and 95, as non-isotopic ions (Fig. 3) (non-isotopic ions are those that only contain  $^{12}\text{C}$  and  $^1\text{H}$ , not  $^{13}\text{C}$  or  $^2\text{H}$ ). Only mass 81 has previously been reported as a monoterpene fragment in PTR-MS [7,15]. Since signals of ions derived from  $^{13}\text{C}$  monosubstituted molecules must also be considered when calculating VOC concentrations with PTR-MS, each ion signal is expressed as a percentage of the total signal of all ions derived from both non-isotopic and  $^{13}\text{C}$  monosubstituted molecules of the target compounds. Mass 67 accounted for less than 1% of the total ion signal for all the monoterpenes at normal experimental conditions. Mass 95 was also less than 1% of the total ion signal, except in the case of limonene (5%). The protonated molecular ion (mass 137) at normal conditions was 43–49% of the total for  $\alpha$ - and  $\beta$ -pinene and limonene. On the other hand, 3-carene was found to yield a higher relative abundance of mass 137 (57%). However, as the drift tube  $E/N$  value was decreased the percentage of the total signal of mass 137 and 138 (the protonated molecular ions of the non-isotopic and  $^{13}\text{C}$  monosubstituted molecules)

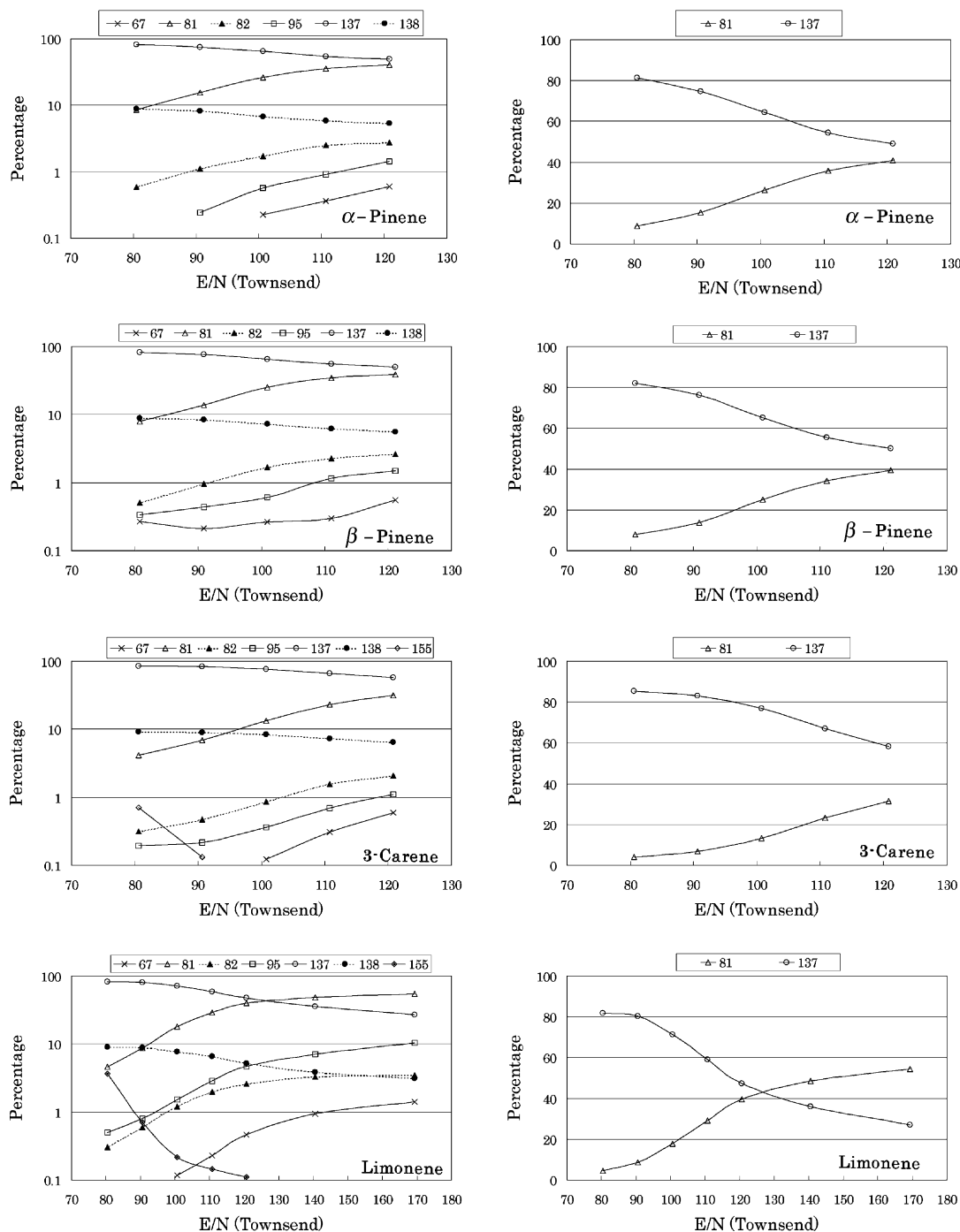


Fig. 3. Fragment patterns of ions derived from  $\alpha$ - and  $\beta$ -pinene, 3-carene, limonene, *p*-cymene and camphor as affected by  $E/N$ , shown as a percentage of total ion signal. Left figures include major ions derived from the neutral, shown on a log scale. Right figures show fragment patterns of the dominant ions as a percentage of the total signal of all ions derived from the neutral, shown on a linear scale. Each data point is the mean of 10–20 determinations.



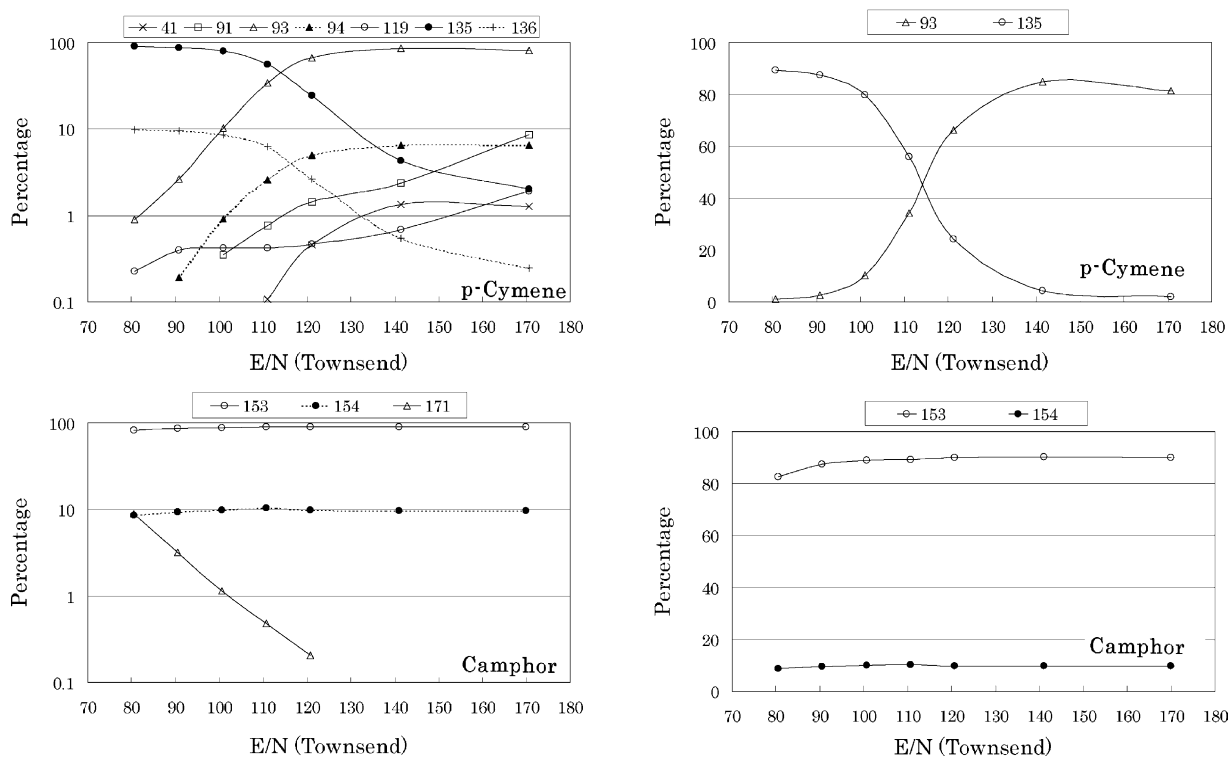


Fig. 3. (Continued).

increased, for each monoterpene, reaching 90–94% at  $E/N$  of 80 Td. In addition to fragment ions, limonene and 3-carene produced monohydrate ions at low  $E/N$  values. This feature is discussed in further detail below.

*p*-Cymene was found to produce unique fragment ions, at masses 41, 91, 93 and 119. Mass 93 was ~70% of the total ion signal at a drift tube  $E/N$  of 120 Td, which was approximately three times as much as that of the protonated molecular ion at mass 135. However, the signal of mass 93 decreased significantly as drift tube  $E/N$  was decreased, representing less than 1% of the total ion signal at an  $E/N$  of 80 Td. In contrast, the signal of protonated molecular ions at masses 135 and 136 increased to over 99% of the total across the same range. The oxygenated monoterpene, camphor, was not observed to yield any fragment ions during PTR-MS analysis, whilst its protonated monohydrate ion ( $C_{10}H_{16}O \cdot H^+ \cdot H_2O$ ) increased in abundance as drift tube  $E/N$  was decreased.

The PTR-MS measurement must be regarded as the sum of indistinguishable VOCs possessing the same molecular weight, such as the monoterpenes. When calculating total monoterpene concentration from the PTR-MS signal, the concentration can be considered as the sum of the signals of masses 67, 68, 81, 82, 95, 96, 137 and 138, and, depending on compounds, 155 and 156. However, we now know the fragment patterns as affected by  $E/N$  and, therefore, we can calculate the sum from the signal of the protonated molecular ion at mass 137 only. The relative abundance of this protonated ion is 0.47, 0.49, 0.43 and 0.58 for  $\alpha$ -pinene,  $\beta$ -pinene, limonene and 3-carene, respectively, at the normal measurement conditions. For the specific application of PTR-MS to measuring monoterpene emissions from trees, knowing that trees release mostly (>60%)  $\alpha$ - and  $\beta$ -pinene and limonene [14], the mean value of the relative abundance of the protonated non-isotopic molecular ion, 0.46, is

recommended as a representative value for biogenic monoterpene flux measurements by PTR-MS. The exception to this would be for tree species known to emit significant quantities of other monoterpene species. The relative abundance of the protonated non-isotopic molecular ion is 0.25 and 0.90 for *p*-cymene and camphor, respectively. Since mass 93 is also the protonated molecular ion of the ubiquitous VOC toluene, it may be unwise to use this mass to quantify *p*-cymene concentrations. In cases where toluene contamination might be expected, quantification using the signal of mass 135 alone is reasonable for providing an estimate of the *p*-cymene concentration. When plants are physically damaged they emit (*Z*)- and (*E*)-hexenal [13] which have a dominant fragment ion of mass 81. Hence mass 137 may give a better estimate of the total monoterpene concentration in this case. Since the signal of protonated  $^{13}\text{C}$  monosubstituted ions in these compounds is  $\sim 11\%$  of that of the protonated non-isotopic ions and, therefore, is less precise, they should be used only as reference ions for the identification of carbon number of the compounds of interest.

From this experiment, it is clear that the monoterpenes  $\alpha$ - and  $\beta$ -pinene, 3-carene and limonene have fragment ions of masses 67 and 95, in addition to mass 81, whilst *p*-cymene produces ions of masses 41, 91, 93 and 119. Information on the fragment patterns is particularly important for the determination of VOC emissions from plants, decaying vegetation and soils using enclosure or cuvette methods. Since monoterpene emissions are often dominant among the emission constituents in these cases, the presence of monoterpene fragment ions might lead to a misidentification or overestimation of other compounds having the same mass as monoterpene molecular or fragment ions.

There have been only a few papers published to date concerning monoterpene emissions from plants measured with PTR-MS [7,15]. Using a dynamic Teflon enclosure technique, masses 67, 93, 95 and 135, as well as masses 81 and 137, were identified in emissions from *Quercus ilex* L., a monoterpene emitting Mediterranean oak species [7]. Although the authors considered toluene emissions to be the source

of a signal detected at mass 93 (without GC-MS verification), a partial or complete contribution from a fragment ion of *p*-cymene must be considered, since *Q. ilex* L. is a known emitter of *p*-cymene (e.g. [14]). Furthermore, the protonated non-isotopic molecular ion of *p*-cymene, mass 135, was also detected, with an ion signal 20–40% of that of mass 93. This ratio is similar to that measured for pure *p*-cymene in our experiments. The authors also attributed masses 67 and 95 to *c*-pentadiene and vinylfuran plus phenol, respectively, with some uncertainties. However, these masses might be fragment ions of monoterpenes, because the signals of masses 67 and 95 were identified to be 1 and 3% of the signal of masses 81 + 137 in all their measurements, with a strong correlation between them. These ratios are also close to those measured for pure monoterpenes in our experiments.

The abundance of monohydrate ions of protonated limonene ( $\text{C}_{10}\text{H}_{16}\cdot\text{H}^+\cdot\text{H}_2\text{O}$ ) and camphor ( $\text{C}_{10}\text{H}_{16}\text{O}\cdot\text{H}^+\cdot\text{H}_2\text{O}$ ) were found to be elevated at low drift tube  $E/N$  values. Varying water vapour pressure in the sample air flow at low  $E/N$  levels provided useful information for identifying what processes brought about this phenomenon. Fig. 4A shows how the signals of ions  $\text{H}_3\text{O}^+$  (mass 19),  $\text{H}_3\text{O}^+\text{H}_2\text{O}$  (mass 37), and  $\text{H}_3\text{O}^+(\text{H}_2\text{O})_2$  (mass 55) in the drift tube were affected by water vapour pressure, at a drift tube  $E/N$  of 80 Td. The signal of the  $\text{H}_3\text{O}^+$  ion decreased as water vapour pressure was increased from 0.6 to 2.4 kPa. The signal of the  $\text{H}_3\text{O}^+\text{H}_2\text{O}$  ion, which was the dominant primary ion at this  $E/N$  value, increased within the lower water vapour pressure range ( $<1.2$  kPa) and then decreased. The signal of the  $\text{H}_3\text{O}^+(\text{H}_2\text{O})_2$  ion, on the other hand, increased with the increase in water vapour pressure across the whole humidity range. As a result of ionic dissociations within the collisional dissociation chamber (CDC) of the PTR-MS, the abundances of  $\text{H}_3\text{O}^+$  and associated water cluster ions measured at the instrument detector are not truly representative of concentrations in the drift tube. However, the low  $E/N$  [11] together with the low drift tube pressure [16] is likely to suppress such ionic dissociations. The measured distribution, therefore, is presumably not significantly different from the true distribution

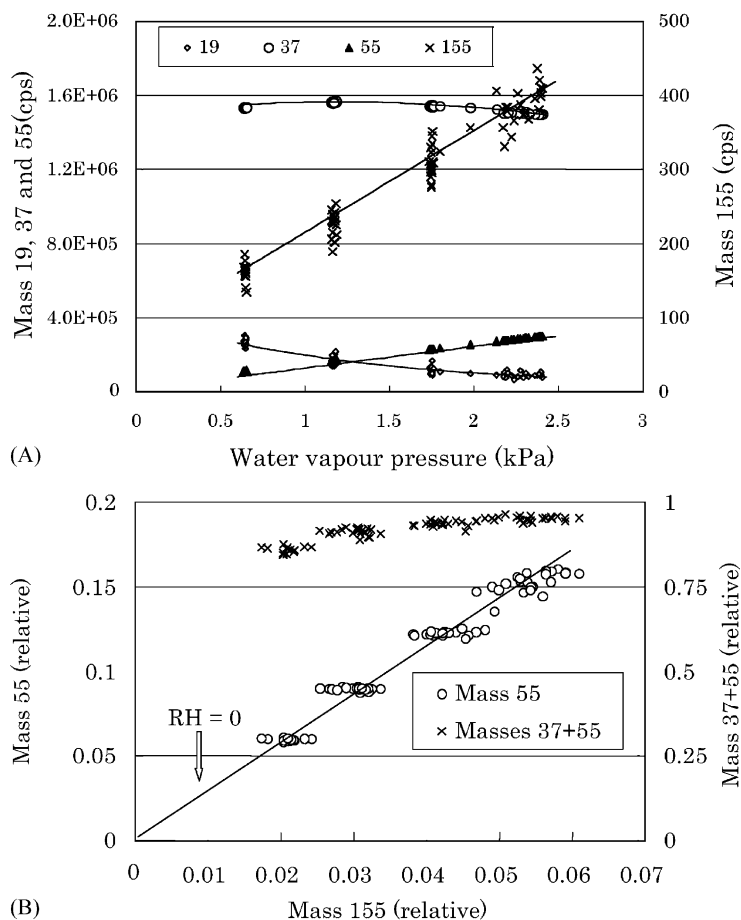
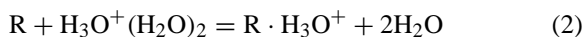


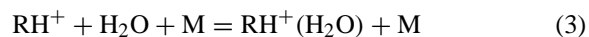
Fig. 4. Signals of masses 19, 37, 55 and 155 derived from limonene as affected by water vapour pressure (A) and the relationship between the hydrated proton donors and mass 155 (B), at  $E/N$  of 80 Td;  $n = 87$ . Masses 37 + 55 and 55 signals in (B) are expressed as signal abundance relative to total signal of proton donors (19 + 37 + 55). Mass 155 signal in (B) is expressed as signal abundance relative to total signal of all ions originated from limonene.

in the drift tube. The abundance of mass 155 also varied with water vapour pressure and was linearly related to the  $\text{H}_3\text{O}^+(\text{H}_2\text{O})_2$  ion, but not with the sum of  $\text{H}_3\text{O}^+\text{H}_2\text{O}$  and  $\text{H}_3\text{O}^+(\text{H}_2\text{O})_2$  ions (Fig. 4B). This result suggests that the monohydrate molecular ions of limonene and camphor may be formed by their respective reactions with the  $\text{H}_3\text{O}^+(\text{H}_2\text{O})_2$  ion.



Since a linear relationship between the signal of the monohydrate ions of the compounds and water vapour

pressure was found (Fig. 4A), another possibility is a three body association reaction given by:



The likelihood of the occurrence of reaction (3) increases as drift-tube  $E/N$  ratio decreases since the reaction is more frequent at lower kinetic energy. If it is assumed that monohydrate molecular ions are formed exclusively via reaction (2), it is possible to estimate the rate coefficient  $k$  for this reaction. If  $k$  is found to be much higher than the estimated reaction rate

coefficient range  $2.4 \times 10^{-9}$  to  $4.4 \times 10^{-9} \text{ cm}^3 \text{ s}^{-1}$ , it is likely to be spurious, which would suggest that reaction (3) is the dominant route by which monohydrate ions of limonene and camphor are produced. This is not the case, however, as is shown in Fig. 4B, where the rate coefficient can be roughly estimated to be two-fifths (reciprocal of the slope of the linear regression between mass 155 and 55) of that for the reaction between  $\text{H}_3\text{O}^+\text{H}_2\text{O}$  and limonene. It is, therefore, difficult to determine whether reaction (2) or (3) is dominant in producing the monohydrate ions, from the limited data obtained with the commercially available PTR-MS instrument.

### 3.2. Rate coefficient calculation

From the toluene measurement, we obtained a traverse time for  $\text{H}_3\text{O}^+$  in the drift tube  $t = 103 \times 10^{-6} \text{ s}$ , which is comparable with the value  $t = 101 \times 10^{-6} \text{ s}$  calculated from the  $\text{H}_3\text{O}^+$  ion mobility value of  $2.8 \text{ cm}^2 \text{ V}^{-1} \text{ s}^{-1}$  measured in nitrogen buffer gas at a  $E/N$  of  $\sim 120 \text{ Td}$  [11]. This similarity indicates

that the whole measurement system is exceptionally accurate. Furthermore, the uncertainty with which proton transfer reaction rate coefficients are determined can be decreased. To calculate the rate coefficients, we used the  $t$  value obtained from our toluene measurement.

Fig. 5 shows the relationship between the concentrations of  $\alpha$ -pinene, camphor,  $p$ -cymene and toluene measured with GC-FID and the sum of signals of all ions derived from individual compounds (including  $^{13}\text{C}$  monosubstituted molecules) simultaneously measured with PTR-MS. The signal was standardised to  $1 \times 10^6 \text{ cps}$  of the proton donors and 2.0 mbar of the drift tube pressure, because small differences in these values occurred between individual experiments. Good linear relationships were observed in all cases ( $r^2 = 0.98\text{--}1.00$  for  $n = 7\text{--}12$ ). The differences in slopes for  $\alpha$ -pinene, camphor,  $p$ -cymene and toluene in Fig. 5 seem to indicate differences in their proton transfer reaction rate coefficients. However, it must be noted that toluene reacts with  $\text{H}_3\text{O}^+$  but not with  $\text{H}_3\text{O}^+(\text{H}_2\text{O})_n$  ( $n \geq 1$ ) whereas monoterpenes react

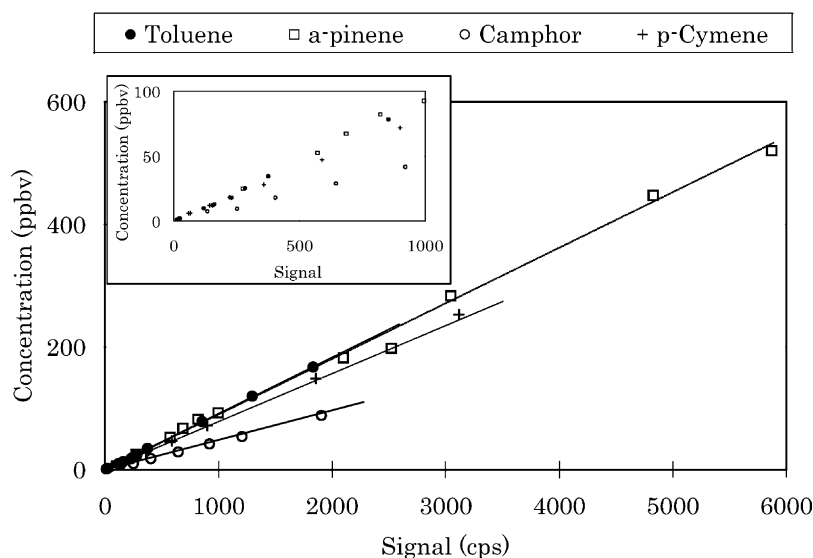


Fig. 5. Relationship between the concentrations of  $\alpha$ -pinene, camphor,  $p$ -cymene and toluene measured with GC-FID and the total *signal* of all ions derived from them. The count rate was standardised to  $1 \times 10^6 \text{ cps}$  of  $\text{H}_3\text{O}^+$  for toluene and  $1 \times 10^6 \text{ cps}$  of  $\text{H}_3\text{O}^+$  plus  $\text{H}_3\text{O}^+\text{H}_2\text{O}$  for the monoterpenes, and 2.0 mbar of the drift tube pressure. Linear regression for each data set were:  $\alpha$ -pinene,  $y = 0.0892 \times x$ ,  $r^2 = 0.998$ ,  $n = 11$ ;  $p$ -cymene,  $y = 0.0808 \times x$ ,  $r^2 = 1.000$ ,  $n = 9$ ; camphor,  $y = 0.0455 \times x$ ,  $r^2 = 0.998$ ,  $n = 8$ ; toluene,  $y = 0.0912 \times x$ ,  $r^2 = 1.000$ ,  $n = 11$ .

with both  $\text{H}_3\text{O}^+$  and  $\text{H}_3\text{O}^+\text{H}_2\text{O}$ . The relationship between  $[\text{R}]$  and  $[\text{RH}^+]$  for the monoterpenes can be approximately expressed as follows:

$$[\text{RH}^+] = \{[\text{H}_3\text{O}^+] + [\text{H}_3\text{O}^+\text{H}_2\text{O}]\}[\text{R}]k_{\text{average}}t_{\text{average}} \quad (4)$$

where  $t_{\text{average}}$  and  $k_{\text{average}}$  are the average traverse time and average reaction rate coefficient weighted for  $\text{H}_3\text{O}^+$  and  $\text{H}_3\text{O}^+\text{H}_2\text{O}$ , respectively. This therefore means that  $t_{\text{average}}$  for the monoterpene reaction differs from  $t$  for the toluene reaction. Under normal drift tube conditions, the signal of  $\text{H}_3\text{O}^+\text{H}_2\text{O}$  measured with the PTR-MS detector, which is placed at the downstream of the drift tube and CDC, is less than 3% of that of  $\text{H}_3\text{O}^+$ , and the signal of  $\text{H}_3\text{O}^+\text{H}_2\text{O}$  in the drift tube, calculated according to Kebarle et al. [17], is less than 5% of that of  $\text{H}_3\text{O}^+$ . Although the ion mobility of  $\text{H}_3\text{O}^+\text{H}_2\text{O}$  is lower than that of  $\text{H}_3\text{O}^+$ , the calculated average ion mobility of  $\text{H}_3\text{O}^+$  plus  $\text{H}_3\text{O}^+\text{H}_2\text{O}$  is only slightly lower than that of  $\text{H}_3\text{O}^+$  alone (the difference is <1%). Therefore, no correction was made for the value of  $t$ . The value of  $k_{\text{average}}$  is also different from  $k$  (as used in Eq. (1)). Since the  $k_{\text{L}}$  and  $k_{\text{C}}$  values for the reaction between mass 136 and  $\text{H}_3\text{O}^+\text{H}_2\text{O}$  are calculated to be 24% less than those for their reactions with  $\text{H}_3\text{O}^+$  [8], owing to a change in reduced

mass, a 1.2% difference between  $k$  and  $k_{\text{average}}$  is estimated at the  $i(\text{H}_3\text{O}^+\text{H}_2\text{O})$  fraction of 5%. Since  $k_{\text{average}}$  was directly obtained from this measurement,  $k$  was corrected according to this difference.

The reaction rate coefficient  $k$  for monoterpene species and  $p$ -cymene is experimentally determined to be in the range  $2.2 \times 10^{-9}$  to  $2.5 \times 10^{-9} \text{ cm}^3 \text{ s}^{-1}$ . Camphor, on the other hand, has a higher rate coefficient of  $4.4 \times 10^{-9} \text{ cm}^3 \text{ s}^{-1}$ . This value is, however, the same as the calculated collisional rate coefficient (Table 1). Since most monoterpene emitting tree species release mostly (>60%)  $\alpha$ - and  $\beta$ -pinene and limonene [14], the mean value of their proton transfer reaction rate coefficient,  $2.3 \times 10^{-9} \text{ cm}^3 \text{ s}^{-1}$ , is appropriate as a representative value.

### 3.3. Effect of water vapour on fragment pattern

Water vapour pressure had a negligible effect on the ion fragmentation patterns of  $\alpha$ - and  $\beta$ -pinene and camphor. The ion pattern of  $p$ -cymene, however, was significantly affected, with the relative abundance of protonated non-isotopic molecular ion increasing from 23 to 31% following a relative humidity change from 26 to 100% at 21 °C (Fig. 6). The ionic patterns of limonene and 3-carene also showed a humidity effect

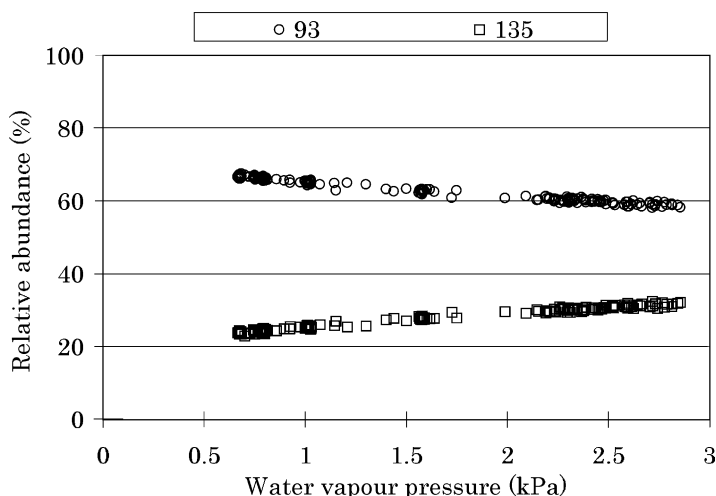


Fig. 6. Relationship between water vapour pressure and abundance of individual ion signals relative to the total signal of all ions deriving from  $p$ -cymene.

on their protonated molecular ion fractions, exhibiting a slight increase with increasing water vapour pressure. These results are consistent with their fragment pattern being changed by a decrease in drift tube  $E/N$  value, by approximately 2–3 Td, as was the case with the humidity change from 0 to 100% (see Fig. 3). This is the case for all compounds used in the present study. However, a change in  $E/N$  is not the cause of these particular changes in fragmentation patterns since  $E/N$  is defined only by the electric field in the drift tube and the number density of the buffer gas, and not by water vapour pressure. As a result,  $E/N$  is constant regardless of humidity. It is therefore reasonable to assume that the average  $KE_{ion}$  for reactions between both neutrals and  $H_3O^+$ , and neutrals and  $H_3O^+H_2O$ , have undergone a slight change ( $<0.01$  eV), as the  $H_3O^+H_2O$  density in the drift tube has changed. The ion mobilities of the two proton donors were estimated to be slightly decreased as water vapour pressure is increased, according to Blanc's law. In addition, the fraction of  $H_3O^+H_2O$ , which has a lower ion mobility, in the drift tube was observed to increase as water vapour pressure was increased and consequently the average ion mobility underwent a slight decrease. Since  $KE_{ion}$  is calculated from ion mobility, the ion mobility change would account for this phenomenon. However, some uncertainty still exists in the fragmentation patterns resulting from the reactions between these neutral compounds and  $H_3O^+H_2O$ . The sum of signals of all ions derived from the standards was also slightly affected by water vapour pressure, because of the change in  $t_{average}$ , which is also affected by the

mean ion mobility. However, these fluctuations were less than 2% and within the instrument precision range [18], and as such need not be considered.

When measuring monoterpene and *p*-cymene concentrations with PTR-MS, as mentioned in the previous section, it might be wiser to use the protonated non-isotopic molecular ion signal only for calculation. In this case, this value must be corrected for water vapour pressure. The correction equation and the corrected fractions at relative humidities of 0 and 100% are shown in Table 2.

#### 3.4. Comparison of concentrations measured with PTR-MS and GC-FID during plant wounding experiments

Count rates of ions derived from monoterpenes increased soon after the Sitka spruce branch was wounded (Fig. 7). They increased again when the water bath temperature was increased from 30 to 50 °C. Strong correlations were found between ions indicative of monoterpene fragments throughout the experimental period. The change in the signal of the protonated non-isotopic ion of the oxygenated monoterpene (mass 153), however, was different from that of the monoterpenes, particularly for the 20 min period following the wounding treatment (i.e., it reached a maximum concentration more slowly than did mass 137).

When calculating the total monoterpene concentration in the glass vessel, the ion signal of mass 137 only was used. The fraction of protonated non-isotopic

Table 2  
Effect of water vapour pressure on relative abundance of protonated non-isotopic molecular ion of compounds in monoterpene family

Molecule	Relative abundance of protonated non-isotopic molecular ion $f(x)$		
	Equation ( $x$ = water vapour pressure, kPa)	At 0% RH	At 100% RH
$\alpha$ -Pinene ( $C_{10}H_{16}$ )	$f(x) = 0.005x + 0.472$	0.47	0.48
$\beta$ -Pinene ( $C_{10}H_{16}$ )	$f(x) = 0.486$	0.49	0.49
Limonene ( $C_{10}H_{16}$ )	$f(x) = 0.017x + 0.419$	0.42	0.46
3-Carene ( $C_{10}H_{16}$ )	$f(x) = 0.011x + 0.565$	0.56	0.59
<i>p</i> -Cymene ( $C_{10}H_{14}$ )	$f(x) = 0.038x + 0.214$	0.21	0.31
Camphor ( $C_{10}H_{16}O$ )	$f(x) = 0.899$	0.90	0.90

Ambient temperature: 21 °C.

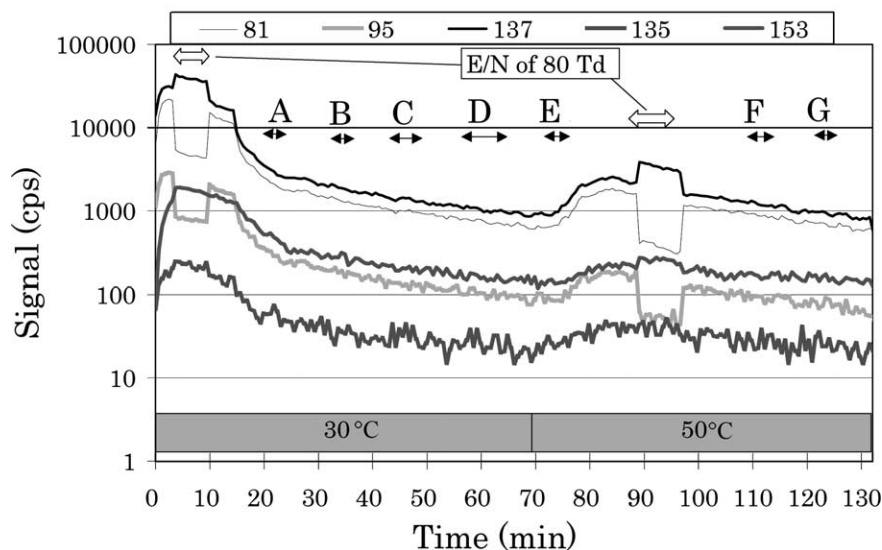


Fig. 7. Changes in ion signals during Sitka spruce wounding experiment. The periods identified with capital letters (A–G) indicate the gas sampling durations for GC-MS analysis.

molecular ion and the mean rate coefficient were assumed to be 0.46 and  $2.3 \times 10^{-9} \text{ cm}^3 \text{ s}^{-1}$  respectively, as described before. The difference in concentrations measured with PTR-MS and GC-FID was less than 20% (Table 3), except for the periods of A and E shown in Fig. 7, during which the signal of mass 137 increased or decreased rapidly.

Although two oxygenated species of formula  $\text{C}_{10}\text{H}_{16}\text{O}$  (camphor and 3-methyl-6-(1-methylethyl)-2-cyclohexen-1-one) and one other compound of mass 152 (2-hydroxy-eozoicacid-methylester) were

identified with GC-MS, the values appropriate for camphor were used for the relative abundance of protonated non-isotopic molecular ion and for the rate coefficient, i.e., 0.90 and  $4.4 \times 10^{-9} \text{ cm}^3 \text{ s}^{-1}$  respectively. Relatively good agreement was found between the two measurements in spite of the low concentrations. PTR-MS analysis tended to underestimate the total concentration of the mass 152 compounds compared with the GC-FID measurements, with most differences in the range 20–50%, except for the period A. For *p*-cymene, concentrations were calculated

Table 3  
Comparison in concentrations of monoterpenes, mass 152 compounds and *p*-cymene measured with PTR-MS and GC-FID

Gas sampling period	Monoterpenes			Mass 152 compounds			<i>p</i> -Cymene			
	PTR-MS <sup>a</sup> (ppbv)	GC-FID (ppbv)	PTR-MS <sup>a</sup> /GC-FID	PTR-MS <sup>a</sup> (ppbv)	GC-FID (ppbv)	PTR-MS <sup>a</sup> /GC-FID	PTR-MS <sup>a</sup> (ppbv)	PTR-MS <sup>b</sup> (ppbv)	GC-FID (ppbv)	PTR-MS <sup>b</sup> /GC-FID
A	196	140	1.41	8.2	7.2	1.15	6.1	1.5	0.3	4.4
B	137	116	1.18	5.4	6.6	0.82	4.0	1.1	0.3	3.7
C	100	87	1.14	4.0	5.2	0.76	3.5	0.8	0.2	4.3
D	73	67	1.09	3.0	4.2	0.73	2.7	0.6	–	–
E	148	160	0.93	3.6	7.5	0.48	4.0	0.9	–	–
F	76	76	1.01	3.1	4.3	0.71	2.6	0.6	–	–
G	61	61	1.00	2.8	3.7	0.76	2.3	0.4	0.1	3.4

Superscript letters (a, b) mean that the concentrations were calculated from the count rate of the protonated non-isotopic molecular ion mass 135, 137 or 153.



in two ways, the first utilising the signal of the protonated non-isotopic molecular ion at mass 135 and the other the fragment ion at mass 93. A correction for the humidity effect was also made. The concentration measured with GC-FID was in the range from 0.13 to 0.39 ppbv. The concentrations calculated from the signal of mass 135 and mass 93, however, were 2.3–6.1 ppbv and 0.4–1.5 ppbv respectively, showing large differences between GC-FID and PTR-MS measurements, and between both PTR-MS measurements.

The uncertainties associated with PTR-MS measurement include those related to the use of mean values for the proton transfer reaction rate coefficients and for the relative abundance of protonated non-isotopic molecular ion produced for the compounds of interest. GC-MS and GC-FID analyses showed that the major monoterpene species emitted from Sitka spruce were  $\alpha$ - and  $\beta$ -pinene, limonene and myrcene, whilst minor compounds were camphene, 3-carene,  $\alpha$ -phellandrene, and  $\alpha$ - and  $\gamma$ -terpinene. The sum of the concentrations of  $\alpha$ - and  $\beta$ -pinene, 3-carene and limonene was  $\sim 60\%$  of the total concentration of monoterpenes detected. Despite the fact that both the proton transfer reaction rate coefficient and the relative abundance of protonated non-isotopic molecular ion produced were unknown for  $\sim 40\%$  of the total monoterpenes emitted, our PTR-MS analysis showed good agreements with the GC-FID measurement. This indicates that the estimated mean values for the rate coefficients and for the relative abundance of protonated non-isotopic molecular ion produced were reasonable, with only a small error.

The largest differences between the two measurement techniques were found for the periods during which drastic changes in ion signals were observed with PTR-MS. It is feasible that this discrepancy is caused by the “sticky” characteristics of the monoterpene compounds. The flow rate of air introduced into the PTR-MS was  $11.8 \text{ mL min}^{-1}$ , whilst that for GC-FID preconcentration was  $200 \text{ mL min}^{-1}$ . Since it is impossible to completely prevent the adsorption of these “sticky” compounds onto the inner surface of the PFA tubing, which was used for all sampling lines in this experiment, considerably more time is

taken for PTR-MS sampling lines to reach adsorptive equilibrium. This may explain why larger concentration differences were observed during periods of rapid concentration change.

The underestimation for the concentration of mass 152 by PTR-MS is probably due to erroneous mean values being assigned to the relative abundance of protonated non-isotopic molecular ion and the proton transfer reaction rate coefficient. Camphor accounted for 37–45% of the total oxygenates, so that these unknown parameters for the other two compounds significantly contributed to the concentration calculation. The concentration measured with PTR-MS would increase if these compounds had produced some fragment ions and/or their rate coefficients had been lower than that of camphor. When quantifying these three compounds of mass 152 by GC-FID, the calibration curve for camphor was used. The use of this for the other two compounds might result in some uncertainties.

For *p*-cymene measurement, we must consider the errors associated with both PTR-MS and GC-FID analyses. The amounts of *p*-cymene sampled onto the adsorbents were close to the detection limit of the GC-FID method. The error associated with this analysis is estimated to be 30%. Two percent of the sum of peak areas in the GC chromatogram could not be identified with GC-MS. There is, therefore, a possibility that another VOC of mass 134 was emitted. PTR-MS measurement for *p*-cymene, on the other hand, includes a larger uncertainty. Monitoring the ratio of mass 93 to the protonated non-isotopic molecular mass 135, and decreasing  $E/N$ , yield useful information on this. The ratio of the signals of mass 93 to mass 135 for *p*-cymene should lie in the range 2–3, but the value during the wounding experiment was 1–1.5. The signal of mass 135 should increase by a factor of 3–4 with a drift tube  $E/N$  change from 120 to 80 Td, if *p*-cymene alone was contributing to the signal at this mass. However, the observed increase was less than 50% in our measurements, suggesting that ions derived from other compounds, either protonated molecular or fragment ions, were included in these ion signals. The ratio of the signals of mass

137 to 81, on the other hand, should be in the range 1.2–1.3 if a monoterpene source is to be suspected. Our measured ratio was 1.3–1.4. In addition, the signal of mass 137 should increase by a factor of 1.5–1.8 with a drift tube  $E/N$  change from 120 to 80 Td. Our measured increase was 1.5–1.7. These results indicate that most of the signal recorded at mass 137 was derived from monoterpene emissions, as verified by GC-MS/FID analysis.

#### 4. Conclusion

From these experiments, it was found that the monoterpenes  $\alpha$ - and  $\beta$ -pinene, 3-carene and limonene produce non-isotopic fragment ions of masses 67, 81 and 95 in the PTR-MS, whilst *p*-cymene produces fragment ions of masses 41, 91, 93 and 119. The fragmentation patterns were affected by  $E/N$  (80–120 Td) and the fragmentation was significantly suppressed at the lowest  $E/N$  value (80 Td). The relative abundance of protonated non-isotopic molecular ion produced was 0.47, 0.49, 0.43, 0.58, 0.25 and 0.90 of the total ion signal for  $\alpha$ -pinene,  $\beta$ -pinene, limonene, 3-carene, *p*-cymene and camphor, respectively, at  $E/N$  of 120 Td. Camphor was not observed to yield any fragment ions within the  $E/N$  range 80–120 Td.

The proton transfer reaction rate coefficient for monoterpene species and *p*-cymene was experimentally determined to be in the range  $2.2 \times 10^{-9}$  to  $2.5 \times 10^{-9} \text{ cm}^3 \text{ s}^{-1}$ . Camphor, on the other hand, gave a higher value of  $4.4 \times 10^{-9} \text{ cm}^3 \text{ s}^{-1}$ . Since most monoterpene emitting tree species release mostly (>60%)  $\alpha$ - and  $\beta$ -pinene and limonene, the mean value of their three proton transfer rate coefficients,  $2.4 \times 10^{-9} \text{ cm}^3 \text{ s}^{-1}$ , is recommended for use when studying biogenic monoterpenes with PTR-MS. Similarly, it is appropriate to use a mean value of 0.46 for the relative abundance of protonated non-isotopic molecular ion produced by biogenic monoterpenes.

The ion pattern of *p*-cymene was significantly affected by water vapour pressure in the sample air. The abundance of its protonated non-isotopic molecular ion relative to the total ion signal increased from 23 to

31% following a relative humidity change from 26 to 100% at 21 °C. Significant water vapour effects were also found for limonene and 3-carene, for which the relative abundance of protonated molecular ion exhibited an increase with increasing water vapour pressure, whilst negligible effects of water vapour were found for  $\alpha$ - and  $\beta$ -pinene and camphor.

Using these reaction data, concentrations of monoterpenes, oxygenated monoterpenes (mass 152) and *p*-cymene were calculated, during a plant wounding experiment, from their protonated non-isotopic molecular ion signals. The differences in total monoterpene concentration measured with PTR-MS and GC-FID were less than 20% in most cases, over the range 60–160 ppbv, indicating that the estimated values used for the mean rate coefficient and relative abundance of protonated non-isotopic molecular ion were reasonable. For mass 152 compounds, PTR-MS underestimated concentrations by ~30%, in most cases, relative to GC-FID, presumably due to inadequate mean values assigned to the relative abundance of protonated non-isotopic molecular ion and the proton transfer reaction rate coefficient (camphor accounted for 37–45% of mass 152 during this experiment). *p*-Cymene concentrations measured by PTR-MS were three times greater than those measured by GC-FID. However, the signal ratio of mass 93 to 135 in the sample air measured with PTR-MS was significantly lower than that for *p*-cymene, suggesting that ions derived from other compounds, either protonated or fragment, were included in these ion signals, erroneously raising the *p*-cymene concentration.

Plants emit many kinds of compounds, including isoprene, the hexenal and hexanal families, monoterpenes, oxygenated monoterpenes of composition  $\text{C}_{10}\text{H}_{16}\text{O}$  and  $\text{C}_{10}\text{H}_{18}\text{O}$ , and sesquiterpenes. The results presented here demonstrate that proton transfer to some of these compounds results in significant and complex fragmentation at the conditions pertaining to PTR-MS analysis. This can easily lead to misidentification of individual compounds in samples of unknown composition. However, by varying  $E/N$  and water vapour concentration in the instrument it is possible to gain additional information that may

aid in compound identification and quantification. For the analysis of mixtures of complex molecules by PTR-MS, simultaneous analysis by GC-FID/MS remains essential.

## Acknowledgements

This work was funded by the Natural Environment Research Council, grant GR3/12750.

## References

- [1] R. Fall, in: C.N. Hewitt (Ed.), *Reactive Hydrocarbons in the Atmosphere*, Academic Press, New York, 1999 (Chapter 5).
- [2] F. Fehsenfeld, J. Calvert, R. Goldan, A.B. Guenther, C.N. Hewitt, B. Lamb, S. Liu, M. Trainer, H. Westberg, P. Zimmerman, *Global Biochem. Cycles* 6 (1992) 389.
- [3] W. Lindinger, A. Hansel, A. Jordan, *Int. J. Mass Spectrom. Ion Processes* 173 (1998) 191.
- [4] C. Warneke, J. Kuczynski, A. Hansel, A. Jordan, W. Vogel, W. Lindinger, *Int. J. Mass Spectrom. Ion Processes* 154 (1996) 61.
- [5] C. Warneke, C. van der Veen, S. Luxembourg, J.A. de Gouw, A. Kok, *Int. J. Mass Spectrom.* 207 (2001) 167.
- [6] R. Holzinger, B. Kleiss, L. Donoso, E. Sanhueza, *Atmos. Environ.* 35 (2001) 4917.
- [7] R. Holzinger, L. Sandoval-Soto, S. Rottenberger, P.J. Crutzen, J. Kesselmeier, *J. Geophys. Res.* 105 (2000) 20573.
- [8] T. Su, W.J. Chesnavich, *J. Chem. Phys.* 76 (1982) 5183.
- [9] R.D. Nelson Jr., D.R. Lide Jr., A.A. Maryott, *CRC Handbook of Chemistry*, CRC Press, Cleveland, OH, 1991.
- [10] V.G. Anicich, *J. Phys. Chem. Ref. Data* 22 (1993) 1469.
- [11] I. Dalton, D.L. Albritton, W. Lindinger, M. Pahl, *J. Chem. Phys.* 65 (1976) 5029.
- [12] S. Hayward, R.J. Muncey, A.E. James, C.J. Halsall, C.N. Hewitt, *Atmos. Environ.* 35 (2001) 4081.
- [13] R. Fall, T. Karl, A. Hansel, A. Jordan, W. Lindinger, *J. Geophys. Res.* 104 (1999) 15963.
- [14] C. Geron, R. Rasmussen, R.A. Arnts, A. Guenther, *Atmos. Environ.* 34 (2000) 1761.
- [15] C. Warneke, T. Karl, H. Judmaier, A. Hansel, A. Jordan, W. Lindinger, P.J. Crutzen, *Global Biogeochem. Cycles* 13 (1999) 9.
- [16] Y.K. Lau, S. Ikuta, P. Kebarle, *J. Am. Chem. Soc.* 104 (1982) 1462.
- [17] P. Kebarle, S.K. Searles, A. Zolla, J. Scarborough, M. Arshadi, *J. Am. Chem. Soc.* 89 (1967) 6393.
- [18] S. Hayward, C.N. Hewitt, J.H. Sartin, S.M. Owen, *Environ. Sci. Technol.* 36 (2002) 1554.